Original Article

Proteomics Study on the Differentially Expressed Proteins in c-fos-silenced Cells Exposed to $PM_{2.5}$*

CAI Ying[1,2,&], ZHENG Kai[1,2,&], LI Run Bing[1,2,&], YU Shu Yuan[2], LIU Ning[2], JI Jia Jia[2], YANG Chen[2], WU De Sheng[2], QIN Shuang Jian[2,3], LI Bo Ru[2,3], ZHANG Zhao Hui[1,#], and XU Xin Yun[2,#]

1. School of Public Health, University of South China, Hengyang 421001, Hunan, China; 2. Institute of Environment and Health, Shenzhen Center for Disease Control and Prevention, Shenzhen 518055, Guangdong, China; 3. Xiangya School of Public Health, Central South University, Changsha 410078, Hunan, China

Abstract

Objective To investigate the effect of c-fos gene silencing on differentially expressed proteins (DEPs) in human bronchial epithelial (HBE) cells after exposure to fine particulate matter ($PM_{2.5}$).

Methods HBE cells and c-fos-silenced HBE cells were exposed to 50 μg/mL $PM_{2.5}$, LC-MS/MS and tandem mass tag (TMT) labeling methods were combined with bioinformatics methods, and DEPs and interaction networks were identified.

Results In the HBE group, 414 DEPs were screened, of which 227 were up-regulated and 187 down-regulated. In the c-fos silenced HBE group, 480 DEPs were screened, including 240 up-regulated proteins and 240 down-regulated proteins. KEGG annotations showed that DEPs in the HBE group are mainly concentrated in the glycolysis/gluconeogenesis pathway and those in the c-fos silenced group are concentrated mainly in endoplasmic reticulum and the processing of proteins. Additionally, the abnormal expression of GPRC5C, DKK4, and UBE2C was identified in top 15 DEPs. After constructing the protein interaction network, 20 Hub proteins including HNRNPA2B1, HNRNPL, RPS15A, and RPS25 were screened from the HBE group and the c-fos silenced HBE group.

Conclusion c-fos gene affected the expression of cancer-related proteins. Our results provided a scientific basis for further study of $PM_{2.5}$-induced carcinogenesis mechanism.

Key words: $PM_{2.5}$; Human bronchial epithelial cells; Gene silence; Proteomics; Bioinformatics

Biomed Environ Sci, 2020; 33(9): 680-689 *doi: 10.3967/bes2020.089* *ISSN: 0895-3988*

www.besjournal.com (full text) *CN: 11-2816/Q*

INTRODUCTION

Air pollution is a recognized risk factor for human health; atmospheric fine particulate matter $PM_{2.5}$ is considered to be the culprit of haze weather[1]. With the rapid growth of China's economy in recent years, most of our population has been exposed to an environment with $PM_{2.5}$[2] exceeding the levels reported in World Health Organization (WHO) air quality guidelines[3,4]. Because $PM_{2.5}$ is classified as a human carcinogen by the international agency for research on cancer (IARC), air pollution has also become a public health problem to be solved urgently in our country. A

*This project was supported by the programs of Shenzhen Science and Technology Innovation Committee to XU Xin Yun [JCYJ20170413101713324, JCYJ20190807102205480]; Shenzhen Key Medical Discipline Construction Fund [SZXK067].

&These authors contributed equally to this work.

#Correspondence should be addressed to XU Xin Yun, Tel: 86-755-25609527, E-mail: xyxu2008@163.com; ZHANG Zhao Hui, Tel: 86-734-8281375, E-mail: zhaohuizzh@126.com

Biographical notes of the first authors: CAI Ying, female, born in 1995, MPH, majoring in environmental toxicology; ZHENG Kai, male, born in 1994, MPH, majoring in environmental toxicology; LI Run Bing, female, born in 1996, MPH, majoring in environmental toxicology.

number of epidemiological investigations and experiments have proved that $PM_{2.5}$ can enter the alveoli and the blood circulation through breathing; therefore, it is closely related to the higher incidence of human respiratory and cardiovascular diseases[5-6]. Therefore, it is particularly important to study the toxicological effects of $PM_{2.5}$ on the lungs to reveal the relationship between air pollution and human health.

As a major substance in air pollutants, $PM_{2.5}$ is closely related to human health[7,8]. Many studies have been carried out on respiratory damage caused by $PM_{2.5}$[9]. Lung cancer is a malignant tumor that threatens human life and health. In recent years, the incidence and mortality of lung cancer in China have increased. Many studies have shown that $PM_{2.5}$ exposure causes inflammation, immune system-associated disorders, epigenetic changes[10], and cancer[11,12]. The c-fos gene is a proto-oncogene, which is closely related to tumorigenesis and development and plays an important role in regulating the basic life activities of cells[13,14]. The purpose of this study was to analyze the differentially expressed proteins (DEPs) in normal HBE cells and c-fos gene-silenced cells by proteomics after $PM_{2.5}$ exposure.

In recent years, proteomics has been widely used in many research fields, which also considered a new platform for screening candidate molecular biomarkers[15]. Mass spectrometry-based techniques can quickly provide high-quality protein expression information. Studies have shown that $PM_{2.5}$ causes damage to HBE cells such as oxidative stress, inflammatory response, and DNA damage[16,17], but no report has explored the effect of $PM_{2.5}$ on protein expression via proteomics in HBE cells. Therefore, this study is based on the c-fos silenced HBE cells constructed successfully in our laboratory. Tandem Mass Tag (TMT) labeled protein quantification technology and mass spectrometry technology were combined with bioinformatics to analyze c-fos silenced HBE cells and DEPs after $PM_{2.5}$ exposure and provide a new direction for the molecular mechanism of $PM_{2.5}$ exposure in HBE cells.

MATERIALS AND METHODS

Reagents and Instruments

Human bronchial epithelial cells were purchased from Shanghai China Cell Bank, Dulbecco's Modified Eagle Medium (DMEM) was purchased from Hyclone (USA), and fetal bovine serum (FBS) was purchased from Gibco (USA). Medium flow atmospheric sampler (TH-150C III) was obtained from Wuhan Tianhong Instrument Co., Ltd. Q Exactive mass spectrometer, Ultimate 3000, APC-3000, and TMTsixplex™ Isobaric Label were purchased from Thermo Fisher (USA). TEAB was purchased from Thermo Company and Trypsin/Lys-C Mix and Mass Spec Grade were purchased from Promega. (USA)

$PM_{2.5}$ Sample Collection and Preparation

The medium flow membrane filters were used to collect $PM_{2.5}$ (TH-150F, Wuhan Tianhong Company, China) for 24 h per day in Taiyuan (Shanxi university campus, Taiyuan, Shanxi province, China). $PM_{2.5}$ samples were collected once every three months for three days during 2017–2018. The flow rate was set at 100 L/min. Moreover, quartz fiber membrane filter was applied to collect $PM_{2.5}$. The quartz fiber membrane that adsorbs $PM_{2.5}$ particles was cut into small pieces and dissolved in ultra-pure water with sonication for 30 min. The solution of $PM_{2.5}$ was dried in freeze vacuum for 24 h and then UV-treated for 1 h[18,19]. The $PM_{2.5}$ stock solution was prepared by adding sterile water. It can be used in cell experiments after autoclaving.

Cell Culture and Exposure

The c-fos silenced HBE cells were successfully constructed in our laboratory previously using shRNA lentiviral vectors. The efficiency of c-fos gene silence was revealed to be satisfactory by RT-PCR and western blot. HBE cells and c-fos silenced cells were cultured and passaged in high glucose DMEM (containing 10% newborn bovine serum, 100 U/mL penicillin, 100 μg/mL streptomycin) in a 37 °C, 5% CO_2 incubator. After the cells covered 80%–90% of the bottom of the bottle, they were treated with $PM_{2.5}$ solution at the dose of 50 μg/mL and cultured in high glucose DMEM without serum and antibiotics at 37 °C and 5% CO_2 for 24 h.

Preparation of Protein Samples

Cells exposed to $PM_{2.5}$ were washed thrice with phosphate buffer saline (PBS), followed by addition of trypsin containing ethylene diaminetetraacetic acid (EDTA) and digestion for 7 min in a 37 °C, 5% CO_2 incubator. The cells were gently blown with DMEM containing 10% FBS to stop digestion. They were pipetted into a centrifuge tube and centrifuged at 1,000 rpm for 5 min. The medium was discarded, and 1 mL PBS was added. The solution was

resuspended and centrifuged at 1,000 rpm for 5 min. PBS was discarded. This procedure was repeated twice, and the clean residual PBS was separated. About 200 μL lysate of 8 mol/L urea (protease inhibitor in urea) was added to each tube. To enhance the contact of the cells and lysate, air was blown into the tube. The solution was placed on ice for 15 min after centrifugation and centrifuged again at 4 °C, 12,000 rpm for 15 min. Protein quantification was performed according to the instructions on the BCA protein quantification kit and the solution was stored at -80 °C until usage.

About 150 μg of total protein sample was used for each sample in an ultrafiltration tube, and 500 μL of 10 mmol/L DL-Dithiothreitol (DTT) was added. After centrifugation at 4 °C, 12,000 rpm, for 15 min, the filtrate was discarded in the collection tube. This was repeated thrice and the tubes were incubated at room temperature 25 °C for 1 h. About 400 μL 20 mmol/L Indole-3-acetic acid (IAA) was added at to the tubes, and they were centrifuged at 4 °C, 14,000 rpm for 15 min. The filtrate was discarded in the collection tube (100 μL remaining in the ultrafiltration tube after centrifugation), and the procedure was repeated twice. The tubes were incubated for 1 h in the dark. About 400 μL of 100 mmol/L triethylamineborane (TEAB) was centrifuged at 4 °C, 14,000 rpm for 15 min, and the filtrate was discarded in the collection tube (100 μL remaining in the ultrafiltration tube after centrifugation). This procedure was repeated thrice. The ultrafiltration tube was placed in a new collection tube, centrifuged at 4 °C, 1,000 rpm for 1 min, and the filtrate was collected. Trypsin was added at a ratio of 100:1 (100 μg total protein was added to 1 μg trypsin), and the enzyme were hydrolyzed at 37 °C overnight.

TMT Marking and Sub-components

According to the Thermo Scientific™ TMT™ instruction method, TMT was used to label the digested samples. Each tube was labeled with 1 label, vortexed, and incubated at room temperature for 1 h. About 8 μL of 5% hydroxylamine was added for 15 min at room temperature to terminate the reaction. To evaporate the solution in EP tube after mixing, 2–18 centrifugal concentrator was used. About 0.1% formic acid (FA) was used to dissolve the evaporated samples. The samples were divided into groups using Ultimate 3000 and APC-3000 instruments (Thermo, USA). Each component was evaporated to dryness using a PVC 2–18 centrifugal concentrator.

LC-MS/MS Analysis

The components of the spin-dried samples were dissolved in 20 μL of 0.1% FA, mixed by vortex, and tested using a Q Exactive mass spectrometer. UniProt human database was used to obtain the original data.

Bioinformatics Analysis

Enrichment analysis of differential proteins was performed using the DAVID database (https://david.ncifcrf.gov/). Gene ontology (GO) analysis of differential proteins can be performed based on three aspects (biological processes, cell components, molecular functions). For enrichment, the Kyoto encyclopedia of genes and genomes (KEGG) can reflect the pathways of differential protein participation, and R language (ver 3.5.1) was used to draw a KEGG bubble chart to compare differential proteins. STRING database (https://string-db.org/) was used to predict the interactions between differential proteins. Cytoscape software is a tool that can visualize the network, combining the results of the protein interaction TSV files obtained by STRING to draw differential protein interaction networks map, and screen Hub proteins to further study the significantly affected metabolism and related signal transduction pathways.

Statistics

SPSS 24.0 statistical software was used for statistical analysis. The experimental data is expressed as $\bar{x} \pm s$. Comparison between groups was performed using analysis of variance. LSD-*t* test was used for pairwise comparison. Fisher's exact probability test was used for GO and KEGG enrichment analyses. $P < 0.05$ was considered statistically significant.

RESULTS

Profile analysis of DEPs

The integrated method of LC-MS/MS and TMT labeling was used to analyze the proteomic changes in the $PM_{2.5}$-exposed HBE cells and c-fos silenced HBE cells. The DEPs with post-translational modifications were extracted from the UniprotKB database, and the differential proteins were obtained according to the criteria of $P < 0.05$. The volcano diagram in Figure 1 shows the differential protein expression profile, and the heat map in Figure 1 shows the different distribution of DEPs in

the c-fos silenced HBE group between the experimental group and the control group. According to the criteria of FC ≤ 0.83 or FC ≥ 1.2 and *P* value < 0.05, top 15 differential proteins in the HBE group were selected, of which 6 were up-regulated and 9 down-regulated. Among c-fos silenced HBE groups, 4 proteins were up-regulated and 11 were down-regulated in top 15 DEPs (Tables 1-2).

GO Enrichment Analysis of DEPs

Normal HBE cells and c-fos silenced HBE cells were exposed to $PM_{2.5}$ treatment. The analysis of GO and KEGG annotations showed that HBE group and c-fos silenced HBE group were involved together in the biological processes in which the differential proteins were mainly related with mRNA splicing, via spliceosome, cell–cell adhesion, and translational initiation. The differential proteins in the HBE group are mainly involved in biological processes such as translational elongation, regulation of cellular response to heat, and negative regulation of apoptotic process. The c-fos silenced HBE group is mainly involved in biological processes such as ribosomal small subunit biogenesis, regulation of translational initiation, and cell division. The cellular components of differential proteins in two groups are mainly distributed in extracellular exosome, mitochondrion, ribosome, myelin sheath, and other components. The cellular components of differential proteins in the HBE group were mainly distributed in the spliceosomal complex, catalytic step 2 spliceosome, and lysosomal lumen, whereas in the c-fos silenced HBE group, the differential proteins involved were mainly in the mitochondrial inner membrane and perinuclear region of cytoplasm. The molecular functions of the differential proteins in two groups are mainly involved in poly (A) RNA binding, protein binding, cadherin binding in cell–cell

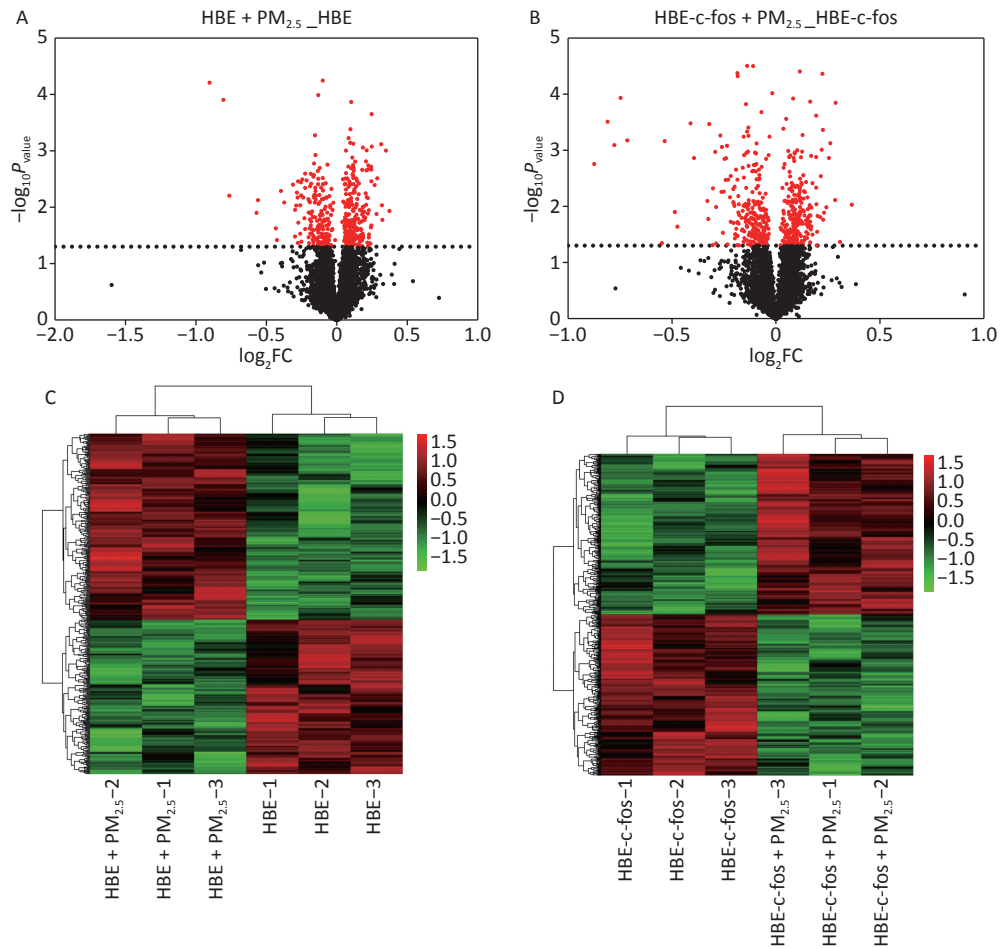

Figure 1. Volcano gram and heat map of proteomics analysis. (A) Volcanic map of $PM_{2.5}$-induced DEPs in HBE cells. (B) Volcanic map of $PM_{2.5}$-induced DEPs in c-fos silenced HBE cells. (C) Heat map of $PM_{2.5}$-induced DEPs in HBE cells. (D) Heat map of $PM_{2.5}$-induced DEPs in c-fos silenced HBE cells.

adhesion, and structural constituent of ribosome. The molecular functions of the differential proteins in HBE group are mainly associated with ubiquitin protein ligase binding, Arp2/3 complex binding, protein kinase binding, and G-protein coupled receptor binding. The molecular functions of the differential proteins in c-fos silenced HBE group were mainly related to translation initiation factor activity, mRNA 3'-UTR binding, and ribosome binding (Figures 2-4).

KEGG Enrichment Analysis of DEPs

KEGG analysis showed that the pathways in which the DEPs in two groups participate together

Table 1. Top 15 differentially expressed proteins in the HBE group

Protein accession number	Protein name	Gene	FC	Up/down	*P* value
Q9NQ84-2	G-protein coupled receptor family C group 5 member C	GPRC5C	1.30	up	0.01
Q92597	Protein NDRG1	NDRG1	1.27	up	< 0.01
O75874	Isocitrate dehydrogenase (NADP) cytoplasmic	IDH1	1.25	up	0.02
O95749	Geranylgeranyl pyrophosphate synthase	GGPS1	1.25	up	0.01
P14324	Farnesyl pyrophosphate synthase	FDPS	1.25	up	< 0.01
P82930	28S ribosomal protein S34, mitochondrial	MRPS34	1.22	up	< 0.01
P02768	Serum albumin	ALB	0.57	down	< 0.01
P02765	Alpha-2-HS-glycoprotein	AHSG	0.59	down	0.01
Q8N257	Histone H2B type 3-B	HIST3H2BB	0.67	down	0.01
Q15004	PCNA-associated factor	PCLAF	0.68	down	0.01
P02774-3	Vitamin D-binding protein	GC	0.74	down	0.02
Q8NI35	InaD-like protein	PATJ	0.75	down	0.04
Q8N2C7	Protein unc-80 homolog	UNC80	0.76	down	0.01
P35237	Serpin B6	SERPINB6	0.77	down	0.01
P13693	Translationally-controlled tumor protein	TPT1	0.81	down	< 0.01

Table 2. Top 15 differentially expressed proteins in the c-fos silenced HBE group

Protein accession number	Protein name	Gene	FC	Up/down	*P* value
Q9UBT3	Dickkopf-related protein 4	DKK4	1.29	up	0.01
P53602	Diphosphomevalonate decarboxylase	MVD	1.24	up	0.04
Q92820	Gamma-glutamyl hydrolase	GGH	1.22	up	< 0.01
O95471	Claudin-7	CLDN7	1.22	up	0.01
Q9Y6V0-5	Protein piccolo	PCLO	0.55	down	< 0.01
P02768	Serum albumin	ALB	0.57	down	< 0.01
P05090	Apolipoprotein D	APOD	0.58	down	< 0.01
Q15004	PCNA-associated factor	PCLAF	0.60	down	< 0.01
P02765	Alpha-2-HS-glycoprotein	AHSG	0.61	down	< 0.01
P02787	Serotransferrin	TF	0.68	down	0.05
Q8N2C7	Protein unc-80 homolog	UNC80	0.69	down	< 0.01
Q8NI35	InaD-like protein	PATJ	0.71	down	0.01
P02788	Lactotransferrin	LTF	0.72	down	0.02
P35237	Serpin B6	SERPINB6	0.75	down	< 0.01
O00762	Ubiquitin-conjugating enzyme E2 C	UBE2C	0.76	down	< 0.01

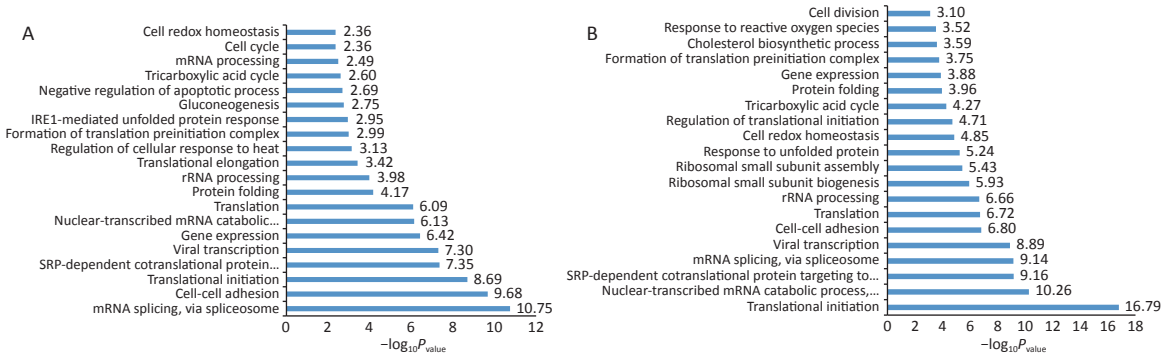

Figure 2. Biological processes of differentially expressed proteins after $PM_{2.5}$ exposure. (A) HBE group. (B) c-fos silenced HBE group.

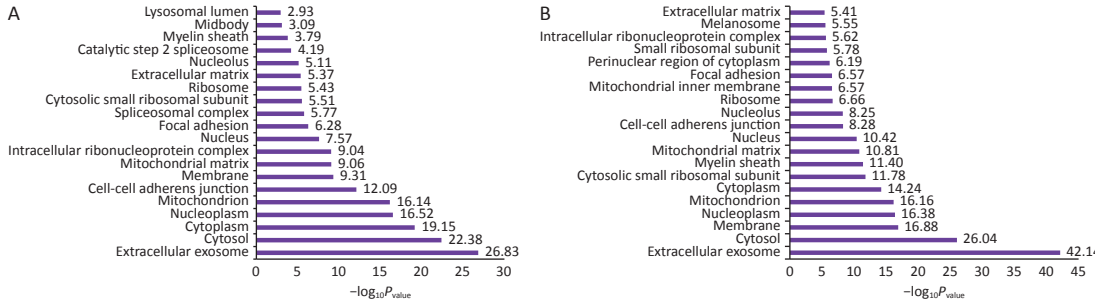

Figure 3. The cell components of differentially expressed proteins after $PM_{2.5}$ exposure. (A) HBE group. (B) c-fos silenced HBE group.

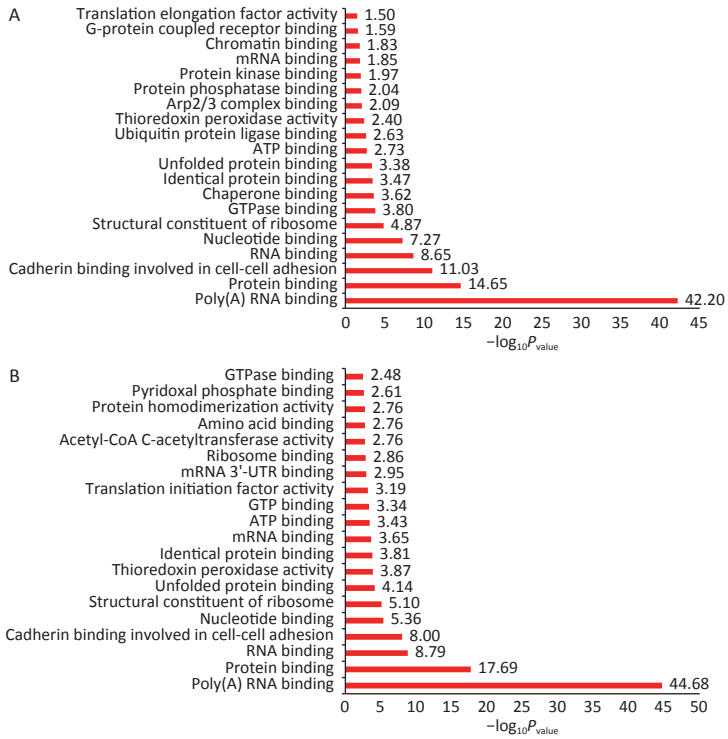

Figure 4. Functional annotation of differentially expressed proteins after $PM_{2.5}$ exposure. (A) HBE group. (B) c-fos silenced HBE group.

are carbon metabolism, ribosome, citrate cycle (TCA cycle), amino acid biosynthesis, and spliceosome. Glycolysis/gluconeogenesis is the only pathway involved in differential proteins in the HBE group. The pathways of differential protein participation in c-fos silenced HBE group include protein processing in endoplasmic reticulum, aminoacyl-tRNA biosynthesis, pyruvate metabolism, lysosome, valine and other pathways (Figure 5).

Protein Interaction Analysis

The STRING database was used to analyze the protein–protein interactions of the screened DEPs. The results were visualized in cytoscape shown in Figure 3A. The Hub network in the two network diagrams is obtained using the cytoHubba plug-in in cytoscape, which is the key protein in the protein interaction network. The Hub proteins in the normal HBE group are HNRNPA2B1, HNRNPA3, RBMX, HNRNPU, SNRPA, HNRNPF, SF3B1, SF3A3, HNRNPL, and ALYREF. In the c-fos silenced HBE group, the Hub proteins were RPS9, RPS21, RPS7, RPS25, RPL31, RPS27A, RPS15, RPS15A, RPS28, and RPL30 (Figure 6, Table 3).

DISCUSSION

In the present study, we used bioinformatics to annotate the HBE group and c-fos silenced HBE group. GO results revealed that c-fos silence can affect biological processes such as apoptosis, protein translation processing, and cell division. KEGG enrichment analysis found that c-fos silence can affect protein processing and lysosome pathways. According to the criteria of FC ≤ 0.83 or FC ≥ 1.2, and $P < 0.05$, top 15 differential proteins such as GPRC5C and NDRG1 in the HBE group were screened, and top 15 differential proteins such as DKK4 and MVD in the c-fos silenced HBE group were screened. Ross identified that GPRC5C expression was continuously elevated in neuroblastoma stem cells[20]. Some studies have found that high glucose can reduce the expression of Wnt signaling pathway antagonist DKK4 and enhance the transport of classic Wnt signaling pathway through Wnt3a ligand-mediated β-catenin to promote the proliferation of liver cancer cells[21]. Related studies have shown that UBE2C can express carcinogenic factors, and its high expression is significantly related to the poor prognosis of breast cancer patients ($P < 0.05$)[22]. Changes in the expression levels of these top 15 differential proteins indicated the functionality and importance of the c-fos gene for the molecular mechanism of $PM_{2.5}$ oncogenesis.

HNRNPA2B1, HNRNPA3, RBMX, HNRNPU, SNRPA, HNRNPF, SF3B1, SF3A3, HNRNPL, and ALYREF were screened from the differential protein interaction network map in the HBE group. HNRNPA2B is an expressed heterogeneous ribonucleoprotein (hnRNP) A/B subfamily. hnRNP are

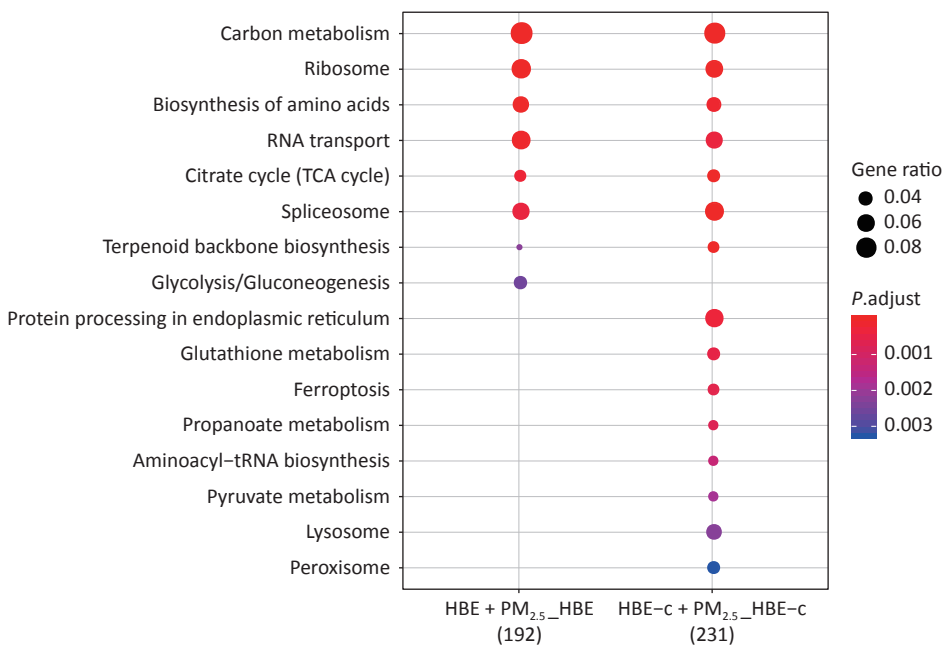

Figure 5. KEGG enrichment analysis of differentially expressed protein after $PM_{2.5}$ exposure.

RNA-binding proteins that form complexes with heterogeneous nuclear RNA (hnRNA). These proteins are associated with pre-mRNA in the nucleus and affect pre-mRNA processing and other aspects of mRNA metabolism and transport, which can affect RNA processing, splicing, transport, and stability of many genes. hnRNPA2/B1 is expressed and promotes the proliferation and metastasis of various cancer types. Yu et al.[23] found that HNRNPA2B1 can be regulated by lncRNA CACNA1G-AS1 to promote the progression of epithelial-mesenchymal transition (EMT) in non-small cell lung cancer (NSCLC) and promote cell invasion and migration capabilities. Ayse studied the toxic effect of silver nitrate on human alveolar basal epithelial cells of A549 adenocarcinoma and found that the down-regulation of HNRNPL gene was identified as an apoptosis-inducing gene and played a certain role in the anti-cancer process[24]. It has been found that inhibition of SF3B1 expression can effectively reduce the proliferation rate of AGS and MKN28 gastric cancer cells by inducing apoptosis and G2/M phase arrest[25]. From the differential protein interaction network diagram of the c-fos silenced HBE group, 10 Hub proteins such as RPS9, RPS21, RPS7, RPS25, RPL31, RPS27A, RPS15, RPS15A, RPS28, and RPL30 were screened. Some studies have found that RPS15A is over-expressed in lung cancer tissues and plays a role as an oncogene in the progression of lung cancer. Reducing its expression can inhibit the malignant progression of lung cancer[26,27]. Studies have found that the expression level of RPS25 in lung

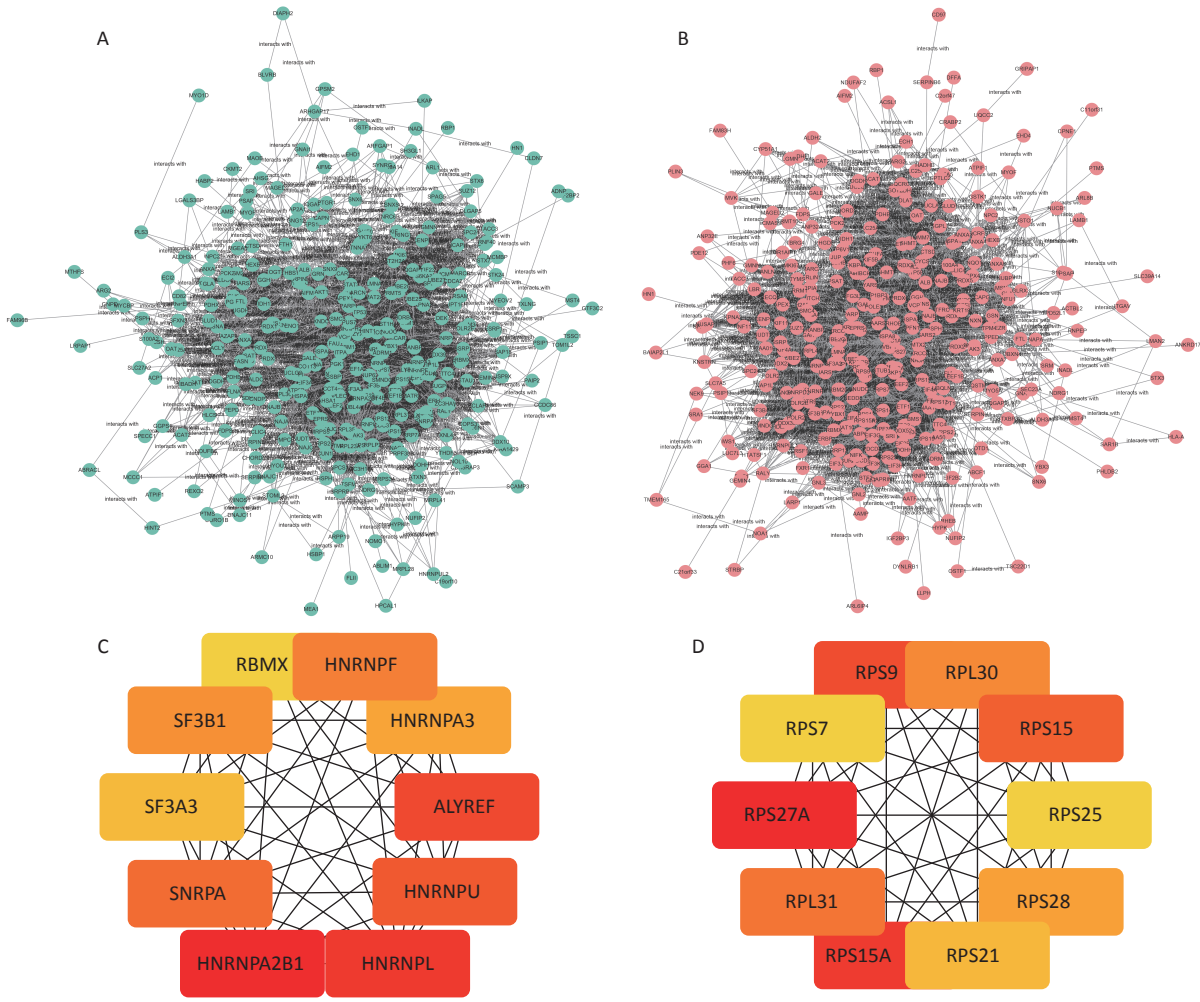

Figure 6. Network diagram of differential protein interactions after $PM_{2.5}$ exposure. (A) Interaction network diagram of differential proteins in HBE group; (B) Interaction network diagram of differential proteins in c-fos silent HBE group; (C) Hub protein network diagram of HBE group; (D) c-fos Hub protein network diagram of HBE group.

adenocarcinoma tissues is significantly higher than that in adjacent normal tissues[28]. Study showed that RPS25-MDM2-p53 regulates the feedback loop to affect the occurrence and development of cancer[29]. Chen et al.[30] found that reduced expression of RPS27a inhibits the proliferation of H8 cell lines by up-regulating Mdm2 phosphorylation on serine residue 166, promoting Mdm2-mediated P53 ubiquitination. Ribosome proteins (RPs) are considered to have the function of ribose in *vitro* and participate in the biological processes of cell growth, division, and apoptosis. This study showed that the Hub proteins screened in the c-fos silenced HBE group were all ribosomal proteins, were rich in the biological processes of the set analysis, and showed a downward regulation trend. The ribosomal protein in the Hub protein in normal HBE group has an upward trend.

In summary, this study preliminary explored the proteomic characteristics of c-fos gene in $PM_{2.5}$-treated HBE cells and showed the biological effects and signal pathways of DEPs in HBE group and c-fos silenced HBE group. Additionally, it revealed that c-fos gene has a certain effect on $PM_{2.5}$-exposed HBE cells and affected the expression of cancer-related proteins. Our results provided a scientific basis for further study of $PM_{2.5}$-induced carcinogenesis mechanism.

Received: March 2, 2020;
Accepted: July 2, 2020

REFERENCES

1. Zhou M, He G, Fan M, et al. Smog episodes, fine particulate pollution and mortality in China. Environ Res, 2015; 136, 396−404.
2. Song C, He J, Wu L, et al. Health burden attributable to ambient $PM_{2.5}$ in China. Environ Pollut, 2017; 233, 575−86.
3. Zhan D, Kwan MP, Zhang W, et al. Spatiotemporal variations and driving factors of air pollution in China. Int J Environ Res Public Health, 2017; 14, 1538.
4. Han L, W Zhou, W Li, et al. City as a major source area of fine particulate ($PM_{2.5}$) in China. Environ Pollut, 2015; 206, 183−7.
5. Kisseleva T, Bhattacharya S, Braunstein J, et al. Signaling through the JAK/STAT pathway, recent advances and future challenges. Gene, 2002; 285, 1−24.
6. Wu Y, Tian Y, Wang M, et al. Short-term exposure to air pollution and its interaction effects with two ABO SNPs on blood lipid levels in northern China: a family-based study.

Table 3. Hub differential proteins in the HBE group and c-fos-silenced HBE group

Group	Abbreviation of protein	Protein name	FC	Up/down
HBE group *vs*. HBE + $PM_{2.5}$ group	HNRNPA2B1	Heterogeneous nuclear ribonucleoproteins A2/B1	1.10	up
	HNRNPA3	Heterogeneous nuclear ribonucleoprotein A3	1.09	up
	RBMX	RNA-binding motif protein, X chromosome	1.09	up
	HNRNPU	Heterogeneous nuclear ribonucleoprotein U	1.07	up
	SNRPA	U1 small nuclear ribonucleoprotein A	1.07	up
	HNRNPF	Heterogeneous nuclear ribonucleoprotein F	1.06	up
	SF3B1	Splicing factor 3B subunit 1	1.06	up
	SF3A3	Splicing factor 3A subunit 3	1.06	up
	HNRNPL	Heterogeneous nuclear ribonucleoprotein L	1.04	up
	ALYREF	THO complex subunit 4	0.83	down
c-fos silenced group *vs*. c-fos silenced + $PM_{2.5}$ group	RPS9	40S ribosomal protein S9	0.87	down
	RPS21	40S ribosomal protein S21	0.89	down
	RPS7	40S ribosomal protein S7	0.90	down
	RPS25	40S ribosomal protein S25	0.92	down
	RPL31	60S ribosomal protein L31	0.92	down
	RPS27A	Ubiquitin-40S ribosomal protein S27a	0.93	down
	RPS15	40S ribosomal protein S15	0.93	down
	RPS15A	40S ribosomal protein S15a	0.94	down
	RPS28	40S ribosomal protein S28	0.94	down
	RPL30	60S ribosomal protein L30	0.98	down

Chemosphere, 2020; 249, 126120.
7. Liu Q, Baumgartner J, Schauer J. Source apportionment of fine-particle, water-soluble organic nitrogen and its association with the inflammatory potential of lung epithelial cells. Environ Sci Technol, Environ Sci Technol, 2019; 53, 9845−54.
8. Liu Q, Baumgartner J, Zhang Y, et al. Oxidative potential and inflammatory impacts of source apportioned ambient air pollution in Beijing. Environ Sci Technol, 2014; 48, 12920−9.
9. Li T, Hu R, Chen Z, et al. Fine particulate matter ($PM_{2.5}$): the culprit for chronic lung diseases in China. Chronic Dis Transl Med, 2018; 4, 176−86.
10. Ning J, Li P, Zhang B, et al. miRNAs deregulation in serum of mice is associated with lung cancer related pathway deregulation induced by $PM_{2.5}$. Environ Pollut, 2019; 254, 112875.
11. Gogna P, Narain TA, O'Sullivan DE, et al. Estimates of the current and future burden of lung cancer attributable to $PM_{2.5}$ in Canada. Prev Med, 2019; 122, 91−9.
12. Li R, Yang L, Jiang N, et al. Activated macrophages are crucial during acute $PM_{2.5}$ exposure-induced angiogenesis in lung cancer. Oncol Lett, 2020; 19, 725−34.
13. Senecal A, Munsky B, Proux F, et al. Transcription factors modulate c-fos transcriptional bursts. Cell Rep, 2014; 8, 75−83.
14. Gutiérrez A, Sambuco L, Álvarez L, et al. Expression of estrogen receptor alpha variants and c-Fos in rat mammary gland and tumors. J Steroid Biochem Mol Biol, 2020; 199, 105594.
15. Li X, W Wang, J Chen, et al. Recent progress in mass spectrometry proteomics for biomedical research. Sci China Life Sci, 2017; 60, 1093−113.
16. Yuan Q, Chen Y, Li X, et al. Ambient fine particulate matter ($PM_{2.5}$) induces oxidative stress and pro-inflammatory response *via* up-regulating the expression of CYP1A1/1B1 in human bronchial epithelial cells *in vitro*. Mutat Res Genet Toxicol Environ Mutagen, 2019; 839, 40−8.
17. Ren X, Tang Y, Sun J, et al. Flavone protects HBE cells from DNA double-strand breaks caused by $PM_{2.5}$. Hum Cell, 2018; 31, 116−26.
18. Liu W, Xu Y, Liu W, et al. Oxidative potential of ambient $PM_{2.5}$ in the coastal cities of the Bohai Sea, northern China: seasonal variation and source apportionment. Environ Pollut, 2018; 236, 514−28.
19. Liu Q, Lu Z, Xiong Y, et al. Oxidative potential of ambient $PM_{2.5}$ in Wuhan and its comparisons with eight areas of China. Sci Total Environ, 2020; 701, 134844.
20. Ross RA, Walton JD, Han D, et al. A distinct gene expression signature characterizes human neuroblastoma cancer stem cells. Stem Cell Res, 2015; 15, 419−26.
21. Chouhan S, Singh S, Athavale D, et al. Glucose induced activation of canonical Wnt signaling pathway in hepatocellular carcinoma is regulated by DKK4. Sci Rep, 2016; 6, 27558.
22. Kim YJ, Lee G, Han J, et al. UBE2C overexpression aggravates patient outcome by promoting estrogen-dependent/independent cell proliferation in early hormone receptor-positive and HER2-negative breast cancer. Front Oncol, 2019; 9, 1574.
23. Yu PF, Kang AR, Jing LJ, et al. Long non-coding RNA CACNA1G-AS1 promotes cell migration, invasion and epithelial-mesenchymal transition by HNRNPA2B1 in non-small cell lung cancer. Eur Rev Med Pharmacol Sci, 2018; 22, 993−1002.
24. Kaplan A, CiftciAG, Kutlu HM. The apoptotic and genomic studies on A549 cell line induced by silver nitrate. Tumour Biol, 2017; 39, 1010428317695033.
25. Zhang Y, Yuan Z, Jiang Y, et al. Inhibition of splicing factor 3b subunit 1 (SF3B1) reduced cell proliferation, induced apoptosis and resulted in cell cycle arrest by regulating homeobox A10 (HOXA10) splicing in AGS and MKN28 human gastric cancer cells. Med Sci Monit, 2020; 26, e919460.
26. Ning Q, Pang Y, Shao S, et al. MicroRNA-147b suppresses the proliferation and invasion of non-small-cell lung cancer cells through downregulation of Wnt/beta-catenin signalling via targeting of RPS15A. Clin Exp Pharmacol Physiol, 2020; 47, 449−58.
27. Zhao X, Shen L, Feng Y, et al. Decreased expression of RPS15A suppresses proliferation of lung cancer cells. Tumour Biol, 2015; 36, 6733−40.
28. Hsu CH, Hsu CW, Hsueh C, et al. Identification and characterization of potential biomarkers by quantitative tissue proteomics of primary lung adenocarcinoma. Mol Cell Proteomics, 2016; 15, 2396−410.
29. Zhang X, Wang W, Wang H, et al. Identification of ribosomal protein S25 (RPS25)-MDM2-p53 regulatory feedback loop. Oncogene, 2013; 32, 2782−91.
30. Chen L, Wang H. Nicotine promotes human papillomavirus (HPV)-immortalized cervical epithelial cells (H8) proliferation by activating RPS27a-Mdm2-P53 pathway *in vitro*. Toxicol Sci, 2019; 167, 408−18.